POLITECNICO
MILANO 1863

SCUOLA DI INGEGNERIA INDUSTRIALE
E DELL'INFORMAZIONE

EXECUTIVE SUMMARY OF THE THESIS

Electronic and atomic structures of iron oxalate dihydrate at extreme conditions

TESI MAGISTRALE IN ENGINEERING PHYSICS– INGEGNERIA FISICA

AUTHOR: FRANCESCA FRULLA

ADVISOR: MARCO MORETTI

CO-ADVISOR: VALERIO CERANTOLA

ACADEMIC YEAR: 2021-2022

1. Introduction

Simple inorganic coordination polymers, such as the iron oxalate, have attracted much interest in the past decades because of their fascinating solid state properties. For these reasons, iron oxalate dihydrate has emerged as an important building block for the preparation of new, functional advanced materials, as an important precursor to the synthesis of materials relevant in geosciences and planetary sciences. Despite extensive investigations carried out, next to nothing is known about the physico-chemical properties of iron(II)oxalate dihydrate at extreme pressures and temperatures. Preliminary results [1] have shown that $FeC_2O_4 \times 2\ H_2O$ exhibits several structural transitions upon pressure increase, which have not yet been characterized. Thus, the aim of this thesis is the investigation of the structural evolution (both electronic and atomic) of $FeC_2O_4 \times 2\ H_2O$ at extreme pressures and its stability at extreme pressures and temperatures.

2. Methods

In this thesis, pre-selected single crystals of $FeC_2O_4 \times 2\ H_2O$ (typical dimensions $15\times15\times10\ \mu m^3$) were characterized by Synchrotron Mössbauer spectroscopy (SMS) at ID18 at ESRF, by X-ray diffraction (XRD) at ID15b at ESRF and by Raman spectroscopy at the Bayerisches Geoinstitute (BGI). We used SMS to study the nuclear and electronic evolution of the material under compression, XRD to study changes in the long-range ordered structure and Raman spectroscopy to study vibrational, rotational and other low-frequency molecular modes.

2.1. Sample preparation

The availability of high-quality single crystals of $FeC_2O_4 \times 2\ H_2O$ is crucial for diffraction or spectroscopic studies at high pressure. Muller et al. [1] describes a versatile synthetic approach to single crystals of $FeC_2O_4 \times 2\ H_2O$ starting from metallic iron. This preparative two-step approach starts with the dissolution of iron in dilute sulphuric acid and subsequent reaction of the

obtained iron(II)sulphate solution with excess dimethyl oxalate under autogenous pressure [1]. All reactions were carried out in thermodynamic equilibrium and produced only the stable α-polymorph.

2.2 SMS

SMS measurements were carried out at the nuclear resonance beamline ID18 at ESRF. The SMS is based on a nuclear resonant monochromator employing pure nuclear reflections of an iron borate ($^{57}FeBO_3$) crystal. The source provides ^{57}Fe resonant radiation at 14.4 keV within a bandwidth of ~ 6 neV and the beam of γ-radiation emitted by the SMS was focused to a ~ 10 x 3.6 μm^2 spot size, fully within the size of the Fe-oxalate crystal. The small cross section of the beam and its high intensity allow for rapid collection of Mössbauer data. The collection time for one spectrum was ~30/45 minutes.

2.3 XRD

Single-crystal XRD experiments were conducted on the ID15b beamline at ESRF (EIGER2 X 9M CdTe (340x370 mm) flat panel detector, X-rays λ=0.41 Å). The synchrotron radiation was focused to a beam size of ~ 6 x 6 μm^2. Single-crystal diffraction data were collected using the rotation method. The cell was rotated around the ω-axis from − 36° to 36° for pressure below 8 GPa and from − 33° to 33° for pressure above 8 GPa. Each XRD dataset took approximately 20 minutes to be collected.

2.4 Raman Spectroscopy

Raman data were acquired at the BGI in Bayreuth (Germany) and Raman spectroscopy was performed using the LabRAM HR system, which excites Raman modes using the 532 nm HeNe green laser with maximum power of 10mW. The scattered radiation was collected and analyzed by the spectrometer Olympus BX40. Raman spectra were collected in different ranges of wavelengths and at different pressure. A spectrum in a wide range (from ~ 200 cm^{-1} to ~ 1700 cm^{-1}) and two shorter ranges (short range 1 from 200 cm^{-1} to 1250 cm^{-1} and short range 2 from 1350-1400 cm^{-1} to 1700 cm^{-1}) were acquired for each pressure point. The first spectra, at lower pressure, were acquired in about 10 minutes and the last spectra, above 50 GPa, took ~ 50 minutes to be collected, due to longer exposure and number of cycles utilized.

3. Results

In order to carry out SMS and XRD experiment at extreme pressures, we used two different membrane cells (DAC1 and DAC2) provided by the ESRF, while to reach extreme temperatures we used the infrared YAG laser installed at ID18 at ESRF. DAC1 was laser heated at T ~ 2000(100) K while DAC2 was laser heated in two different area at T ~ 2400(100) K and T ~ 2950(100) K, respectively. For the Raman experiment, we used the piston-cylinder type BX90 mechanical DAC (DAC3). The samples were loaded in DACs with rhenium gasket and Neon gas was used as pressure-transmitting-medium (PTM) to maintain quasi-hydrostatic conditions during compression. DAC1, that reached 50 GPa, had cullets of 300 μm while DAC2 and DAC3, that reached 100 GPa of maximal pressure, had cullets of 150 μm.

3.1 SMS

Mössbauer spectra were collected at different pressure steps. For DAC1 we only acquired the spectra before and after the laser heating at 50 GPa while for DAC2 we compressed the sample at pressure steps of 4/5 GPa from ambient pressure to 100 GPa and a total of 17 spectra were collected. After laser heating at 100 GPa we measured two more spectra in two different positions of the sample. The Mossbauer spectra were fitted using the software package MossA. The most relevant Mössbauer fittings are shown in Figure 3.1.1; these are the ones obtained by compressing DAC2 before laser heating.

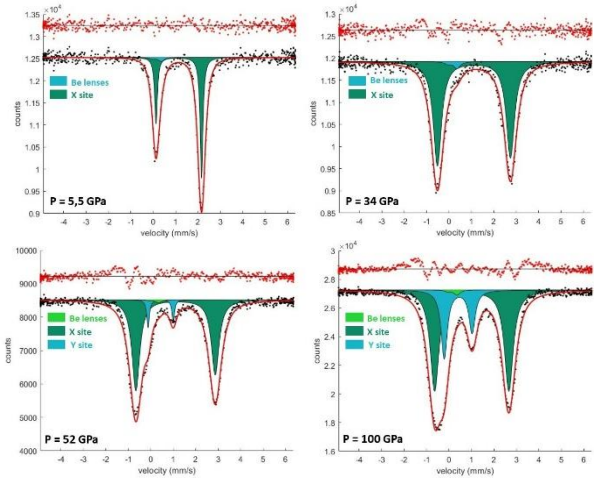

Figure 3.1.1: Mossbauer spectra.

Mössbauer spectra were fitted using Lorentzian lines and the lowest number of components, i.e. one component for the initial X site (green doublet) and one component for the Y site (blue doublet), which appears at around 52 GPa. From Figure 3.1.1 we notice that the spectra measured at low pressure are characterized by only one doublet, then between 17 GPa and 34 GPa a change in the asymmetry of the doublet is observed due to a phase transition (confirmed by XRD and in accordance with the preliminary studies made by Müller et al. [1]), at 52 GPa another doublet starts to appear and at 100 GPa both doublets are still present. From the hyperfine parameters we can affirm that at the beginning, the doublet of the X site (dark green) represents Fe^{2+} in HS state and in octahedral coordination (CS = 1.14 mm/s and QS = 2.03 mm/s at 5.5 GPa), then at P > 22 GPa the phase transition and progressive distortion of the X site create the conditions for the increase of coordination number of to dodecahedral (CS = 1.11 mm/s and QS = 3.57 mm/s at 44 GPa). At 52 GPa another doublet starts to appear, which we attribute to the spin transition of Fe^{2+} in dodecahedral of octahedral coordination from HS configuration to a LS one. Center shift and quadrupole splitting hyperfine parameters are plot at the increase of pressure for the two sites in Figure 3.1.2. We identified, in accordance with XRD data, four different regions representing changes in the atomic and electronic structures, highlighted in Figure 3.1.2 using straight lines of different colors.

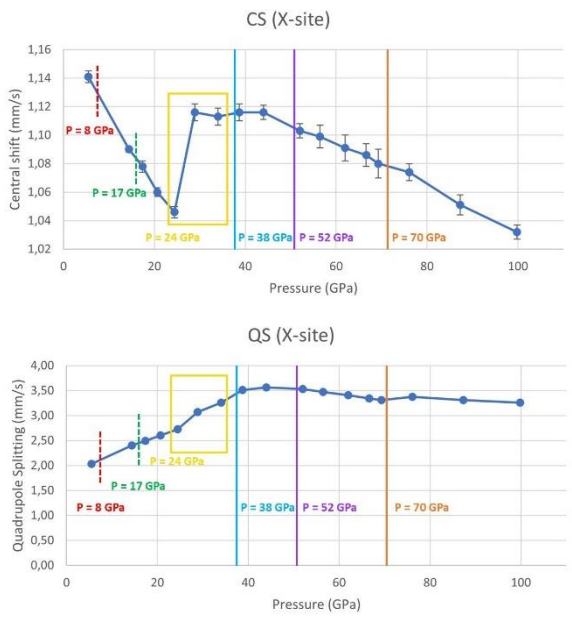

Figure 3.1.2: Evolution of hyperfine parameter.

From Figure 3.1.2 we notice an initial decrease of the CS for the X site at the increase of pressure, which we attribute to the rise of the electron density at the nucleus during compression. Between 24 GPa and 29 GPa there is a jump in the CS from 1.046 mm/s to 1.116 mm/s, which then remains more or less constant until 44 GPa. In this pressure interval, around 38 GPa we observed from XRD data the completion of a sluggish structural transition which started at P > 22 GPa (Fig. 3.1.2). At the appearance of the second doublet at 52 GPa, the CS of both sites start to decrease again. From the evolution of the QS values, we notice that the QS for the X site increases with pressure until ~ 40 GPa, which can be explained by a continuous distortion of the X site and the completion of the phase transition. At the emergence of the second doublet, the value of the QS of X site is more or less stable while the QS of the Y site follow a more complicate path, indicating an increasing trend.

3.2 XRD

The XRD spectra were also collected at different pressures. DAC1 was compressed at pressure steps of 3/4 GPa from ambient pressure to 50 GPa. A total of 17 XRD patterns were collected. After laser heating at 50 GPa we performed again a diffraction measurement on the quenched products. We also acquired the XRD pattern of DAC2 at 100 GPa before and after laser heating. The analysis of the XRD data with CrysAlis^{PRO} program is still in progress. As a preliminary analysis, the diffraction images taken for each different pressure have been merged to obtain a single wide angle image using CrysAlis^{PRO} softwar. In this way we were able to analyze the data as powder diffraction images. A preliminary and qualitative analysis of the wide angle images was made using the software Dioptas. The most relevant XRD pattern are shown in Figure 3.2.1; these are the ones obtained from DAC1 before laser heating.

In the XRD integrated patterns we identified with asterisks the appearance of new peaks, with circles the disappearance of previous peaks and with arrows the evident variations in peaks intensity. Qualitatively, we could locate a first change in the structure at 7.9 GPa, where new peaks emerge and others disappear. This changes however are not in agreement with previous studies [1] and might be generated during the merging method, since we

are treating single crystal data as powders and unwanted effect caused by twinning for instance cannot be avoided. Similarly, other changes observed at ~ 17 GPa are linked to the merging of integrated images from the two different crystallographic domains of the twinned crystal.

At higher pressures instead, I noticed, in accordance with preliminary studies of Müller et al. [1], the evident appearance of new peaks starting at ~ 22 GPa, while reflections from the monoclinic structure get progressively lower in intensity. I interpreted this trend with the coexistence of two structures between 22 GPa and 38 GPa, the monoclinic structure of the oxalate at ambient conditions, observed until 38 GPa, and the high-pressure structure that begins to form at 22 GPa and that is completely formed at 38 GPa, growing at the expenses of the lower pressure one. One should consider however that the progressive distortion of the monoclinic structure can cause a moderate shifts on the scattering angle of some reflections, not resulting however in a complete phase transition. Thus what we observe at 17 GPa might also be seen as a combination between distortion of the original monoclinic structure and twinning effects. I can affirm this because from previous studies [1] it is known that iron oxalate is very compressible and its structure undergoes distortions already at low pressures (~ 10 GPa).

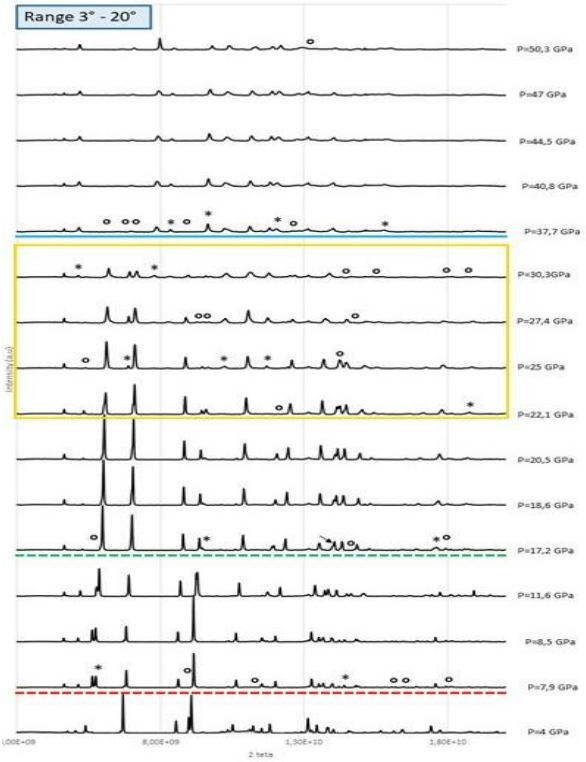

Figure 3.2.1: XRD pattern.

3.3 Raman Spectroscopy

As before, the Raman data were acquired at different pressure steps. The DAC was compressed at pressure steps of 3/4 GPa from ambient pressure to 100 GPa and a total of 20 spectra were collected. The data were analyzed with OriginLab software. In order to do the analysis, I subtracted to all spectra the background. The peaks in the spectra were fitted with a standard Gaussian function and considering all the fittings I obtained an R-squared (R^2) in the range between 0,89 – 0,98. At ambient conditions the sample shows five Raman bands in the region from 200 cm^{-1} to 3500 cm^{-1} (Fig. 3.3.1).

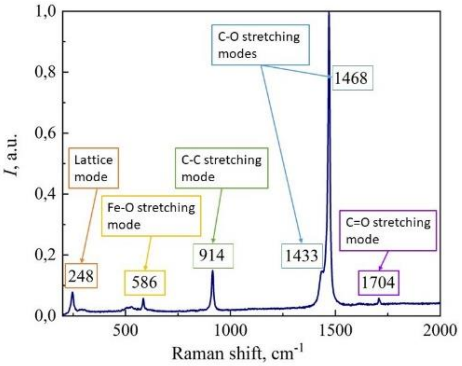

Figure 3.3.1: Raman mode at ambient pressure.

All bands shift to higher frequencies with increasing pressure and at higher pressure new bands start to appear. At 3 GPa the bands characteristic of Fe-oxalate at ambient conditions are still present but the one at 1704 cm^{-1} disappears and one more band appears in the region between 500-600 cm^{-1}. A further increase in pressure to 9 GPa causes several new vibrational modes to appear at lower wavenumbers (lattice mode), a less intense band appears at ~ 840 cm^{-1} and another one appears at ~ 1520 cm^{-1}. The spectral evolution seems to indicate the presence of a phase transition in this pressure interval, as normally the appearance of new Raman bands indicate structural changes or at least the formation of new molecular interactions. However, from Müller et al. [1] and our XRD preliminary analysis, it is known that the structure remains the same until ~ 20 GPa, thus we believe the appearance of new bands are caused by inter-molecular interactions due to strong structural compaction and distortion. Between 16 GPa and 22 GPa there is a clear lowering of the peaks' intensity, which is an evidence of phase transition, in fact above 22 GPa the intensity is recovered. In the same pressure interval and in the region between 1450-1650 cm^{-1} the intensity of the second band at higher

wavenumbers (1564 cm^{-1} at 16 GPa and 1594 cm^{-1} at 22 GPa), starts to decrease. At 25 GPa another mode appears (~ 1537 cm^{-1}) and from 34 GPa it seems that only one broad peak characterize the spectrum, even if one could fit it using more than one component, i.e. more than one gaussian curve. In the mid-frequency range, I noticed that at 22 GPa the intensity of the band identified with number 3 in Figure 3.3.2 drastically decreases and a new band identified with number 1 appears. Between 22 GPa and 25 GPa there is an evident change in the intensity of the two bands, 1 and 2, with peak 1 that grows at the expenses of peak 2, and peak 3 disappear. However, it cannot be excluded that peak 3 (at 959 cm^{-1} at 22 GPa) is no longer distinguishable from the other two (band 1 at 932 cm^{-1} and band 2 at 979 cm^{-1} at 22 GPa) because it merged to peak 1. Then at 34 GPa another band (band 4) appears in the spectrum at 942 cm^{-1} and at 38 GPa band 2 disappears. From 38 GPa to 48 GPa the shape of the spectra remains constant, only the peaks shift to higher wavelengths is observed. At P ~53 GPa the reciprocal intensity of bands 4 and 1 starts to invert (Fig. 3.3.2.a), and complete inversion is reached at ~ 66 GPa, where only a tiny shoulder on the right of band 4 indicate the residual presence of band 1 (highlighted with a light blue arrow in Fig. 3.3.3).

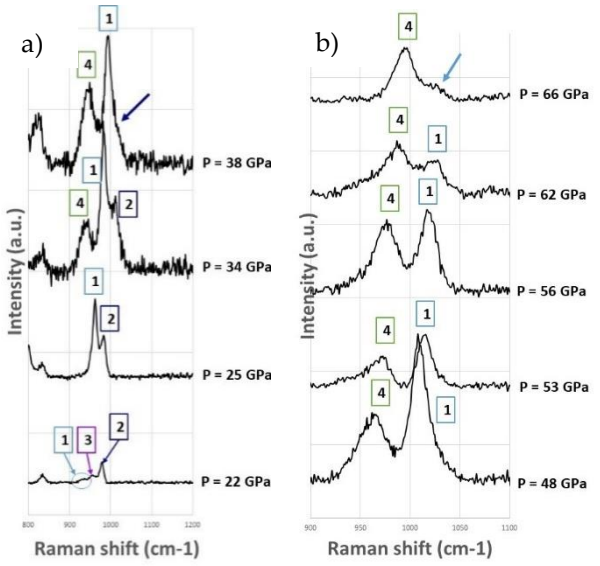

Figure 3.3.2: a) Raman band (800-1000 cm^{-1} / 22-38 GPa) and b) Raman band (800-1000cm^{-1} / 48-66GPa).

4. Discussion

Experiments under extreme conditions are an important tool for synthesis of new materials and investigation of physical and chemical properties of matter in unconventional states. The structural and phase transition of Fe-oxalate dihydrate are already treated in the previous part through the results of SMS, XRD and Raman data (Chapter 3). In the following, I will present some effects the iron oxalate experiences during compression: i) the spin transition and ii) the Jahn-Teller effect. Moreover, I will illustrate the new product synthetized after laser heating.

4.1 Spin transition

The spin transition is a common phenomenon in iron bearing compounds. Fe^{2+} has six electrons in the more external 3d orbitals. The d-orbitals have not the same energy. Indeed, the metal's five degenerate d-orbitals experience specific energy changes when surrounded by certain symmetries of ligands, which act as point charges. The spin crossover arises from a condition in which the thermal energy at high P-T is sufficient to overcome the energy difference between the high-spin and low-spin states [2].

In our Mössbauer spectra, at P > 50 GPa a second doublet (Y site) starts to emerge and grows until P ~ 70 GPa, where the co-existence of the two components appears to reach a steady-state (Fig. 3.1.1). This behavior could be explained by three options: i) transition to a new structure characterized by two distinct iron sites with different coordination numbers and hypothetically different spin states, ii) the pressure induced oxidation of Fe^{2+} to Fe^{3+} or iii) spin pairing of iron 3d electrons (the new doublet is LS Fe^{+2}). The third option is supported by the change in hyperfine parameters (CS of the Y site drops to 0.440(19) mm/s at 52 GPa and QS of Y site has lower values than the QS of X site) and by spin transition observed in ferropericlase and inorganic complexes. Moreover, this option is supported by Raman spectroscopy. Indeed, in the same pressure range, in the region of wavelengths in which C-C symmetric stretching modes and O-C-O bending modes are present (Fig. 3.3.2.b), the intensity of the peak 4 (LS Fe^{+2}) starts to increase until it becomes the dominant peak. The growth of peak 4 at lower frequency could indicate that C-O bonds were pulled, i.e. increase length, caused by the volume collapse of the iron site due to spin crossover, as observed for iron carbonate [3] For these reasons, we attribute the rise of the second doublet (in SMS)

and of peak 4 (in Raman spectroscopy) to the spin transition of iron 3d electrons. However, our interpretation is not yet conclusive, since in the case of spin pairing, one would expect a complete conversion of the first doublet (in SMS) and of the second peak (in Raman spectroscopy), representing iron in a high-spin state, to the advantage of the low-spin doublet, which is not completely fulfilled.

4.2 Jahn-Teller effect

In Raman spectra, Fe^{2+}–O stretching bands are split and broadened in agreement with other studies [4]. Both the broadening and lowering the intensity of the Fe^{2+}–O band may arise from the Jahn-Teller effect of Fe^{2+} ion. In Fe-oxalate, this effect causes the $Fe^{2+}O_6$ polyhedra to be horizontally elongated. The consequence of the Jahn Taller effect is that the coordination environment of Fe^{2+} is a distorted octahedron where the two metal-water bonds (Fe–O3) are shorter than the other four metal-oxalate bonds (Fe–O1 and Fe–O2) that result in the broadening and lowering of the corresponding Raman band. The Jahn-Teller effect also justify the Raman peaks broadening at higher pressures where iron is in a cubic environment, since geometric distortion of the molecule is achieved by distortion of the site and general 3d orbitals degeneracy.

4.3 Synthesis of new products through laser heating

One of the goal of this study was to expose Fe oxalate dihydrate to the extreme conditions of planetary interiors, i.e. the Earth, thus not only high pressures but also temperatures. Through SMS and XRD we confirmed the synthesis of new products at the extreme conditions present inside deep Earth. At 100 GPa and ~ 2750 K we formed an already discovered orthocarbonate $Fe_4C_3O_{12}$ [5] while at 50 GPa and ~2000 K we formed a new tetracarbonate $Fe_5C_3O_{13}$ which may contain OH^- groups in its structure. We also synthesized new other phases as subproducts of the redox reactions. XRD analyses are still ongoing, while a precise characterization of the products using only Mössbauer spectroscopy is not possible without XRD complementary information due to the presence of several iron-bearing compounds in the same spectrum. In $Fe_4C_3O_{12}$ all iron is ferric and there are two structurally distinct iron position. The Fe atom in position 1 is surrounded by nine O atom forming a regular trigonal prism while the Fe atom in position 2 is coordinated to 7 oxygens forming a bicapped trigonal prism. Instead, in $Fe_5C_3O_{13}$ there is a combination of Fe^{2+} and Fe^{3+}. From our results we revealed an already discovered compound containing tetrahedral CO_4 groups ($Fe_4C_3O_{12}$), a new tetracarbonate $Fe_5C_3O_{13}$, which may contain OH group in its structure and the complex role of ferrous and ferric iron in stabilizing carbonates at extreme conditions. These results are important for both the carbon recycle in deep Earth and the deep water cycle in subducting slabs [6].

5. Conclusions and outlook

This thesis was focused on investigating the structural evolution of $FeC_2O_4 \times 2\ H_2O$ under extreme pressures and temperatures. Indeed, iron oxalate is relevant in different research fields such as technology (as anode material for lithium-ion batteries), deep carbon cycle (as precursor of $FeCO_3$) and planetary science (as Fe-C-O phase), thus a complete characterization of its chemical-physical properties in unconventional states is required. Here, we used a set of complementary analytical techniques, XRD, SMS and Raman spectroscopy, to look at the long- and short range ordered structures. The results obtained can be summarized as follows:

i) we determined how many structural / phase transitions happen in $FeC_2O_4 \times 2\ H_2O$ up to 100 GPa and their pressure ranges.

ii) we investigated the amorphization process claimed by Müller et al [1] a P > 20 GPa.

iii) we synthesized new phases relevant for the Earth and icy giants planetary interiors at ~ 50 and ~ 100 GPa and T > 2000 K.

iv) we study the spin crossover in iron atoms at P > 50 GPa.

To finalize this study, more experiments will have to be performed using diamond anvil cells with larger angle opening, i.e. cell aperture of 80° (vs 60° used in the framework of this thesis) in order to collect a higher number of atomic reflections necessary to solve the structures of the newly discovered high-pressure phases. Moreover, X-ray emission spectroscopy experiments are also necessary to confirm the spin transition observed between 52-70 GPa.

References

[1] Müller, H., Bourcet, L., Hanfland, M. (2021). Iron(II)oxalate Dihydrate-Humboldtine: Synthesis, Spectroscopic and Structural Properties of a Versatile Precursor for High Pressure Research. *Minerals*, 11, 113.
[2] Speziale, S., A. Milner, V. E. Lee, S. M. Clark, M. P. Pasternak, and R. Jeanloz. (2005). Iron spin transition in Earth's mantle. *Proc. Natl. Acad. Sci. U.S.A.*, 102
[3] Cerantola, V. et al. (2015.) High-pressure spectroscopic study of siderite ($FeCO_3$) with focus on spin crossover. *Am. Mineral*, 100.
[4] Echigo, T. and Kimata, M. (2008). Single-crystal X-ray diffraction and spectroscopic studies on humboldtine and lindbergite: weak Jahn -Teller effect on Fe^{+2} ion. *Phys Chem Minerals*, 35.
[5] Cerantola, V., Bykova, E., Kupenko, I., Merlini, M., Ismailova, L. (2017). Stability of iron-bearing carbonates in the deep Earth's interior. *Nature Communications*, 8, 9.
[6] Boulard, E., A. Gloter, A. Corgne, D. Antonangeli, A. L. Auzende, J. P. Perrillat, F. Guyot, and G. Fiquet. (2011). New host for carbon in the deep Earth. *Proc. Natl. Acad. Sci. U. S. A.*, 108, 13.

6. Acknowleggements

Thanks to ESRF and BGI for allowing me to do SMS, XRD and Raman experiments. A special thank to all ID18 staff for the help and support during the beamtime and to Valerio Cerantola and Marco Moretti for supervising the realization of this thesis.